

# Microwave zero-resistance states in a bilayer electron system

S. Wiedmann,<sup>1,2</sup> G. M. Gusev,<sup>3</sup> O. E. Raichev,<sup>4</sup> A. K. Bakarov,<sup>5</sup> and J. C. Portal<sup>1,2,6</sup>

<sup>1</sup>*LNCMI-CNRS, UPR 3228, BP 166, 38042 Grenoble Cedex 9, France*

<sup>2</sup>*INSA Toulouse, 31077 Toulouse Cedex 4, France*

<sup>3</sup>*Instituto de Física da Universidade de São Paulo, CP 66318 CEP 05315-970, São Paulo, SP, Brazil*

<sup>4</sup>*Institute of Semiconductor Physics, NAS of Ukraine, Prospekt Nauki 41, 03028, Kiev, Ukraine*

<sup>5</sup>*Institute of Semiconductor Physics, Novosibirsk 630090, Russia and*

<sup>6</sup>*Institut Universitaire de France, 75005 Paris, France*

(Dated: July 9, 2010)

Magnetotransport measurements on a high-mobility electron bilayer system formed in a wide GaAs quantum well reveal vanishing dissipative resistance under continuous microwave irradiation. Profound zero-resistance states (ZRS) appear even in the presence of additional intersubband scattering of electrons. We study the dependence of photoresistance on frequency, microwave power, and temperature. Experimental results are compared with a theory demonstrating that the conditions for absolute negative resistivity correlate with the appearance of ZRS.

PACS numbers: 73.40.-c, 73.43.-f, 73.21.-b

Exposing two-dimensional electron systems (2DES) to a continuous microwave (MW) irradiation in the presence of perpendicular magnetic fields  $B$  has revealed notable “zero-resistance states” (ZRS) for samples with ultrahigh electron mobility and under high MW intensity [1–3]. The longitudinal resistance  $R_{xx}$  vanishes in certain intervals of magnetic fields, whereas the Hall resistance remains unchanged, i.e., does not show plateaus. The ZRS phenomenon is closely related to the microwave-induced resistance oscillations (MIROs) [4] which are governed by the ratio of the radiation frequency  $\omega$  to the cyclotron frequency  $\omega_c = eB/m$ , where  $m$  is the effective mass of the electrons. If the electron mobility is high enough, an increase in MW power transforms the minima of these oscillations to intervals of zero resistance.

In theory, the effect of microwaves on 2DES is described by two microscopic mechanisms. The “displacement” mechanism is based on spatial displacement of electrons along the applied dc field under scattering-assisted microwave absorption [5–7], while the “inelastic” mechanism originates from an oscillatory contribution to the isotropic part of the electron distribution function [8, 9], controlled by inelastic relaxation. Both mechanisms describe phase and periodicity of MIROs observed in experiments, but for low temperatures  $T$  the inelastic mechanism is the dominant one because the inelastic relaxation time  $\tau_{in}$  is large,  $\tau_{in} \propto T^{-2}$ . According to theory [5–8], both mechanisms can lead to negative dissipative resistivity in the MIRO minima with increasing MW power. A direct consequence of negative resistivity (regardless of its microscopic mechanism) is the instability of homogeneous current flow and spontaneous breaking of the sample into a pattern of domains [10]. The simplest domain structure of this kind is viewed as two domains with opposite directions of currents and Hall fields [7, 10]. Each domain is characterized by zero dissipative resistance and classical Hall resistance. A change of the current in this regime is accommodated by a shift of the

domain wall without any voltage drop, so the resistivity becomes zero. More complicated domain structures [11] and an alternative mechanism of ZRS, based on the MW stabilization of the edge-state transport [12], have been proposed recently. Until now, all studies of ZRS are restricted to high-mobility single-layer 2D systems.

Bilayer 2DES, where electrons occupy two closely spaced subbands, exhibit magneto-intersubband (MIS) oscillations of magnetoresistance caused by the periodic modulation of the probability of intersubband transitions by the magnetic field (see Ref. [13] and references therein). In the presence of MW irradiation, the interference of MIROs with MIS oscillations leads to a peculiar magnetoresistance picture with enhancement, suppression, or inversion (flip) of MIS peaks correlated with MW frequency. The photoresistance in bilayers [14] can be described by the inelastic microscopic mechanism at low temperatures. Similar phenomena arise in multisubband systems [15]. However, there is neither experimental nor theoretical evidence for MW-induced ZRS in systems with more than one populated subband. This also raises the question of whether ZRS might be observable in quasi-3D systems.

In this Letter, we present studies of magnetoresistance in a wide quantum well (WQW) exposed to MW irradiation. Owing to charge redistribution, WQWs with high electron density form a bilayer configuration, where the two wells near the interfaces are separated by an electrostatic potential barrier [16], and two subbands appear as a result of tunnel hybridization of 2D electron states. Without microwaves, the magnetoresistance of our system shows MIS oscillations, thereby confirming the existence of two occupied subbands. By applying microwaves, we have found that for different MW frequencies two of the MIS peaks, which are inverted with increasing MW power, evolve into ZRS. Calculations of photoresistance demonstrate that ZRS in our samples appear under conditions for absolute negative resistivity,

which suggests the origin of ZRS as a consequence of current instability.

We have studied 45 nm wide WQWs with high electron density  $n_s \simeq 9.1 \times 10^{11} \text{ cm}^{-2}$ , obtained from the periodicity of Shubnikov-de Haas (SdH) oscillations, and mobility  $\mu \simeq 1.9 \times 10^6 \text{ cm}^2/\text{V s}$ , at  $T = 1.4 \text{ K}$  and after a brief illumination with a red light-emitting diode. The electrons occupy the two lowest subbands, and the corresponding wave functions, symmetric (S) and antisymmetric (AS), are presented in the inset of Fig. 1. The subband separation  $\Delta = 1.40 \text{ meV}$  is extracted from the periodicity of low-field MIS oscillations [13] in agreement with theoretical calculations. The measurements were carried out in a cryostat with a variable temperature insert and a waveguide was employed to deliver linearly polarized MW radiation (frequency range 32.7170 GHz) down to the sample. A conventional lock-in technique was used to measure the longitudinal resistance  $R = R_{xx}$ . The samples have van der Pauw-geometry ( $3 \text{ mm} \times 3 \text{ mm}$ ), and the longitudinal resistance is found to be insensitive to the orientation of the microwave field.

In Fig. 1 we present dark resistance and the observation of a ZRS (marked with an arrow) for 143 GHz at a temperature of 1.4 K. Other MIS peaks, starting from  $B = 0.07 \text{ T}$ , are either inverted or enhanced (since  $\hbar\omega$  is close to  $\Delta/2$ , approximately each second peak in the region above 0.13 T is inverted) but only the MIS peak at 0.27 T exhibits vanishing longitudinal resistance. The resistance without MW irradiation shows MIS oscillations which are superimposed on SdH oscillations for  $B > 0.25 \text{ T}$ . The SdH oscillations are damped due to electron heating by microwaves [14, 15]. The minimum at 0.55 T and weak minima at 0.22 and 0.32 T are not attributed to MIS oscillations. They occur in the regions of transitions from inverted to enhanced MIS, also confirmed by theoretical calculations. The theoretical plot (see details below) shows a negative resistance in the region of experimentally observed ZRS.

Figure 2 illustrates photoresistance in the frequency range from 149 GHz to 100 GHz with four chosen frequencies at 149, 128, 110, and 100 GHz (from top to bottom). We denote the ZRS at  $B = 0.2 \text{ T}$  as peak (I) and the ZRS at  $B = 0.27 \text{ T}$  as peak (II). For all four traces, we show the highest MW intensity (0 dB). As in Fig. 1 for 143 GHz, we observe a ZRS for peak (II) at 149 and 128 GHz. In contrast to  $f \geq 128 \text{ GHz}$ , we find a ZRS for peak (I) at 110 and 100 GHz. Note that the deep minima of ZRS slightly shift to lower magnetic fields as MW frequency decreases (compare 149 with 128 GHz and 110 with 100 GHz). Peak (I), which shows vanishing resistance for 100 and 110 GHz, is strongly enhanced with increasing frequency. The same effect occurs for peak (II), which exhibits ZRS for  $f > 128 \text{ GHz}$  but is first enhanced for 110 GHz and strongly enhanced for 100 GHz. It is worth noting that other MIS oscillations at  $B < 0.2 \text{ T}$  also show enhancement or peak flip correlated with MW frequency but no ZRS. The amplitude of MIS peak at  $B \simeq 0.4 \text{ T}$  becomes smaller with decreasing frequency.

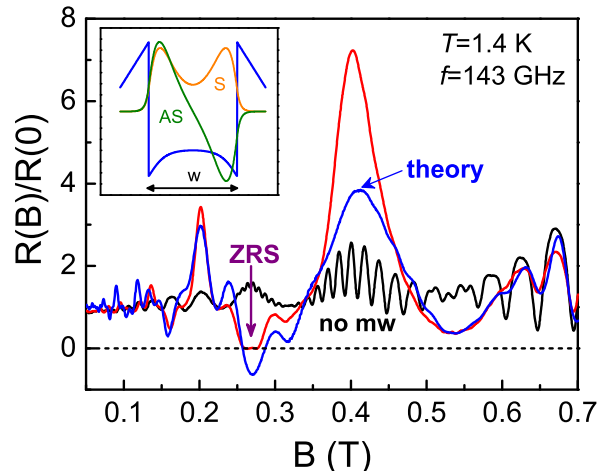


FIG. 1: (color online) Longitudinal resistance without (no MW) and under MW irradiation (143 GHz) at 1.4 K. The microwaves lead to enhancement, suppression, or inversion of the MIS peaks. The inverted MIS peak at 0.27 T exhibits vanishing resistance. These basic features are also seen in the theoretical plot. Inset: WQW with  $w = 45 \text{ nm}$  and corresponding symmetric (S) and asymmetric (AS) wave functions.

The results in Fig. 2 demonstrate the striking difference of ZRS in our bilayer system compared to single-subband systems. In the single-subband systems, MIRO minima evolving into ZRS are placed at  $\omega/\omega_c = j + 1/4$  ( $j$  is integer) and ZRS are observed in a wide frequency range from 7.5 [3] to 240 GHz [17], while in bilayer systems ZRS develop from the strongest minima of combined MIS-MIRO oscillations and their location also depends on subband splitting.

In Fig. 3 we present both power and temperature dependence of magnetoresistance at 143 GHz, when ZRS develops around  $B=0.27 \text{ T}$  with the largest width. In Fig. 3(a) we show power dependence at 1.4 K starting from 0 dB (highest intensity) to  $-10 \text{ dB}$ , as well as the dark magnetoresistance (no MW). With decreasing MW power, the amplitudes of all enhanced and inverted MIS oscillations decrease while ZRS [peak (II)] first narrows and then disappears (at  $-4 \text{ dB}$ ) with decreasing MW power. The temperature dependence in Fig. 3(b) is carried out at a fixed MW power (0 dB, as in Fig. 1), which corresponds to a MW electric field  $E_w \simeq 4.2 \text{ V/cm}$ . The effect of increasing temperature on the amplitudes of magnetoresistance oscillations is similar to the effect of decreasing power. The ZRS starts to narrow at  $T = 2.1 \text{ K}$  and disappears at  $T \simeq 2.5 \text{ K}$ .

Now we analyze power and temperature dependence of  $R(B)/R(0)$  for both MIS peaks transformed into ZRS. In Fig. 4(a) the magnitudes of the enhanced peak (I) and of the inverted peak which evolves into the ZRS (II) are plotted as functions of MW power. For the

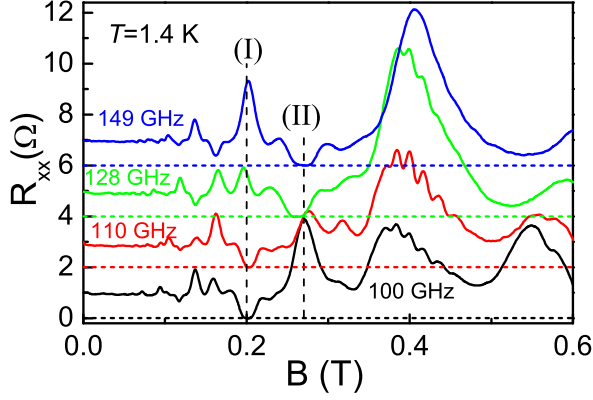


FIG. 2: (color online) Frequency-dependent photoresistance for 149, 128, 110, and 100 GHz exhibits ZRS for two inverted MIS peaks: (I) at 0.2 T and (II) at 0.27 T. Peak (II) is strongly enhanced for 100 GHz but becomes inverted and shows ZRS for 128 and 149 GHz, while peak (I) is enhanced for 149 GHz but shows ZRS for 110 and 100 GHz. Photoresistance traces are shifted up for clarity except for 100 GHz.

enhanced peak (I)  $R_{xx}$  shows a sublinear power dependence before saturation. For the inverted MIS peak (II),  $R_{xx}$  decreases very fast in a narrow power range. The amplitude of the inverted peak [i.e.  $1 - R(B)/R(0)$ ] scales similar to peak (I). Concerning temperature dependence, we observe a strong decrease of  $R(B)/R(0)$  in the low-temperature region, when approaching ZRS. Therefore, we have constructed an Arrhenius plot which is presented in Fig. 4(b) for 143 GHz [ZRS for peak (II)] and 100 GHz [ZRS for peak (I)]. Applying the expression  $R_{xx} \propto \exp(-E_{ZRS}/T)$ , we obtain the activation energy  $E_{ZRS} = 7$  K, which is of the same order as in single-layer systems [1–3]. For higher  $T$ , we see a deviation from the activation dependence, in a similar fashion as in Ref. 3. In the region where the resistivity is not very low [ $R(B)/R(0) > 0.2$ ], the relative change of  $R(B)/R(0)$  with temperature can also be fitted by the dependence  $\propto -T^{-2}$ , for both inverted peaks.

The origin of ZRS is conventionally described in terms of the formation of a domain structure when the resistivity becomes absolutely negative. To check whether a negative resistivity can be reached in our sample under MW excitation, we have calculated the magnetoresistance based on both inelastic and displacement contributions. Calculations reveal that the displacement mechanism becomes essential only for higher MW electric fields and it is justified to neglect its contribution to photoresistance for our experimental conditions. In the regime of classically strong magnetic fields  $\omega_c \tau_{tr} \gg 1$ , where  $\tau_{tr}$  is the transport time, and under a valid condition  $\varepsilon_F \gg \Delta/2$ , where  $\varepsilon_F = \hbar^2 \pi n_s / 2m$  is the Fermi energy ( $\varepsilon_F \simeq 16.3$  meV for our sample), the magnetoresistance

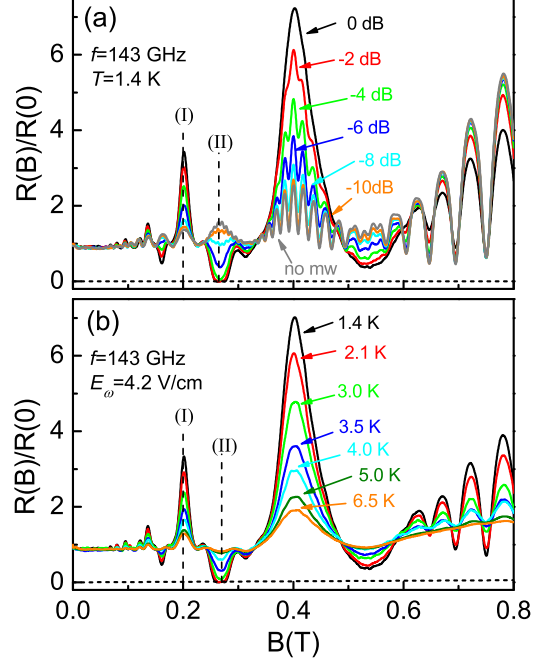


FIG. 3: (color online) (a) Power dependence of magnetoresistance at a constant temperature (1.4 K) and (b) temperature dependence at a constant MW electric field (4.2 V/cm). With decreasing MW power, ZRS disappears at  $-4$  dB and magnetoresistance for peak (II) approaches the dark value for  $-10$  dB. With increasing  $T$ , ZRS also narrows and disappears.

of the balanced double-layer system is expressed as

$$\frac{R(B)}{R(0)} = \int d\varepsilon \left( -\frac{\partial f_\varepsilon}{\partial \varepsilon} \right) \mathcal{D}_\varepsilon^2, \quad (1)$$

where  $f_\varepsilon$  is the distribution function of electrons and  $\mathcal{D}_\varepsilon$  is the dimensionless (expressed in units of  $2m/\pi\hbar^2$ ) density of states. The influence of microwaves on the distribution function is described by the kinetic equation [8, 18]

$$\frac{P_\omega}{4\tau_{tr}} \sum_{\pm} \mathcal{D}_{\varepsilon \pm \hbar\omega} (f_\varepsilon - f_{\varepsilon \pm \hbar\omega}) = -\frac{f_\varepsilon - f_\varepsilon^e}{\tau_{in}}, \quad (2)$$

where the generation term (left-hand side) accounts for single-photon absorption of electromagnetic waves, and the electron-electron collision integral (right-hand side) is written through the inelastic relaxation time  $\tau_{in}$ . Next,  $f_\varepsilon^e$  is the Fermi-Dirac distribution with effective electron temperature  $T_e$  due to heating of the electron gas by microwaves and  $P_\omega \propto E_\omega^2$  is the dimensionless MW power. The density of states for a two-subband system has been calculated numerically by using the self-consistent Born approximation. The quantum lifetime  $\tau_q \simeq 7.1$  ps at 1.4 K ( $\tau_{tr}/\tau_q \simeq 10$ ) is extracted from the amplitudes of MIS oscillations in dark magnetoresistance measurements. The temperature dependence of

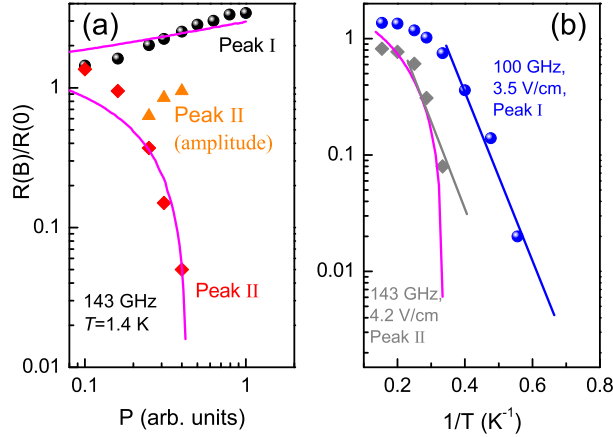


FIG. 4: (color online) Analysis of power and temperature dependence. (a) The normalized magnetoresistance for peak (I) and peak (II), together with relative amplitude of peak (II) for 143 GHz at 1.4 K as a function of MW power. Peak (I) and the amplitude of peak (II) exhibit sublinear power dependence. The magnetoresistance for the inverted peak (II) strongly decreases with increasing MW power. (b)  $R(B)/R(0)$  for 100 GHz [ZRS, peak (I)] and 143 GHz [ZRS, peak (II)]. The straight solid lines are fits to  $R \propto \exp(-E_{ZRS}/T)$ . The curves in (a) and (b) are theoretical plots.

the inelastic relaxation time is taken in the usual form [8]  $\hbar/\tau_{in} = \lambda_{in} T_e^2 / \varepsilon_F$ , where  $\lambda_{in}$  is a numerical constant of order unity. The electron temperature  $T_e$ , which depends on MW power, frequency, and magnetic field, is determined from the balance equation assuming energy relaxation of electrons due to their interaction with acoustic phonons.

The result of calculations based on Eqs. (1)-(2) for 143 GHz and 0 dB attenuation (corresponding MW electric field  $E_\omega = 4.2$  V/cm) with  $\lambda_{in} = 0.5$  is shown in Fig. 1. The theoretical plot in Fig. 1 reproduces all experimentally observed features and shows the negative resistivity around  $B = 0.27$  T [peak (II)]. The calculations for 100 GHz excitation ( $E_\omega = 3.5$  V/cm) also show the negative resistivity around  $B = 0.2$  T [peak (I)]. The power and temperature dependences of the resistance are in reasonable agreement with experiment;

see Fig. 4. In particular, the disappearance of ZRS at  $-4$  dB ( $E_\omega = 2.65$  V/cm) shown in Fig. 3(a) correlates with the results of theoretical calculations.

The deviation of theory from experimental data is probably related to a limited applicability of the relaxation-time approximation [8] in Eq. (2) and to a neglect of confined magnetoplasmon effects on MW absorption [19]. Another source of deviation may be the assumption about homogeneous distribution of the MW field inside the sample and a neglect of the role of contacts or edges. Recently observed insensitivity of MIROs to the sense of circular polarization [20], the absence of MIROs in contactless measurements [21], and theoretical calculations of the MW field distribution in 2DES with metallic contacts [22] indicate the near-contact origin of the phenomena of MIRO and ZRS in high-mobility layers. Since we have used linearly polarized microwaves and have not performed contactless measurements, we cannot definitely say whether a strong MW field gradient near the contacts is important for photoresistance in our bilayers. The absence of clear knowledge about the specific nature of the near-contact oscillating contribution to resistivity [22] does not allow us to discuss this problem in more detail, on the quantitative level.

In conclusion, we have observed ZRS in a high-mobility bilayer electron system exposed to MW irradiation. The manifestation of ZRS in bilayers is distinct from the case of single-layer systems, due to a peculiar magnetotransport picture of a two-subband 2DES, where quantum magnetoresistance is modulated by MIS oscillations. Since the vanishing resistance develops for inverted MIS peaks, the ZRS intervals are narrow, and these states are very sensitive to MW frequency. We do not exclude the possibility that for samples with higher mobility two or more inverted MIS peaks could evolve into ZRS. The observed ZRS can be described as a consequence of current instability under absolute negative resistivity. By demonstrating experimentally that the ZRS phenomenon is not limited to single-layer 2DES, and, theoretically, that the presence of intersubband scattering in bilayers is not an obstacle for the negative resistivity, we suggest that similar physical mechanisms might lead to ZRS in multilayer or quasi-3D electron systems.

This work was supported by CNPq, FAPESP, and with microwave facilities from ANR MICONANO.

- 
- [1] R. G. Mani *et al.*, *Nature* **420**, 646 (2002).
  - [2] M. A. Zudov, R. R. Du, L. N. Pfeiffer, and K. W. West, *Phys. Rev. Lett.* **90**, 046807 (2003).
  - [3] R. L. Willett, L. N. Pfeiffer, and K. W. West, *Phys. Rev. Lett.* **93**, 026804 (2004).
  - [4] M. A. Zudov, R. R. Du, J. A. Simmons, and J. L. Reno, *Phys. Rev. B* **64**, 201311(R) (2001).
  - [5] V. I. Ryzhii, *Sov. Phys. Solid State* **11**, 2078 (1970); V. I. Ryzhii, R. A. Suris, and B.S. Shchamkhalova, *Sov. Phys. Semicond.* **20**, 1299, (1986).
  - [6] A. C. Durst, S. Sachdev, N. Read, and S. M. Girvin, *Phys. Rev. Lett.* **91**, 086803 (2003).
  - [7] M. G. Vavilov and I. L. Aleiner, *Phys. Rev. B* **69**, 035303 (2004).
  - [8] I. A. Dmitriev, M. G. Vavilov, I. L. Aleiner, A. D. Mirlin, and D. G. Polyakov, *Phys. Rev. B* **71**, 115316 (2005).
  - [9] I. A. Dmitriev, A. D. Mirlin, and D. G. Polyakov, *Phys. Rev. B* **75**, 245320 (2007).

- [10] A. V. Andreev, I. L. Aleiner, and A. J. Millis, Phys. Rev. Lett **91**, 056803 (2003).
- [11] I. G. Finkler and B. I. Halperin, Phys. Rev. B **79**, 085315 (2009).
- [12] A. D. Chepelianskii and D. L. Shepelyansky, Phys. Rev. B **80**, 241308(R) (2009).
- [13] N. C. Mamani, G. M. Gusev, T. E. Lamas, A. K. Bakarov, and O. E. Raichev, Phys. Rev. B **77**, 205327 (2008).
- [14] S. Wiedmann *et al.*, Phys. Rev. B **78**, 121301(R) (2008).
- [15] S. Wiedmann *et al.*, Phys. Rev. B **80**, 245306 (2009)
- [16] M. Shayegan *et al.*, Semicond. Sci. Technol. **11**, 1539 (1996).
- [17] R. G. Mani, Appl. Phys. Lett. **92**, 102107 (2008).
- [18] I. V. Pechenezhskii, S. I. Dorozhkin and I. A. Dmitriev, JETP Letters **85**, 86 (2007).
- [19] O. M. Fedorych *et al.*, Intern. Journ. Mod. Phys. **23**, 2698 (2009).
- [20] J. H. Smet *et al.*, Phys. Rev. Lett. **95**, 116804 (2005).
- [21] I. V. Andreev *et al.*, JETP Letters **88**, 616 (2008).
- [22] S. A. Mikhailov and N. A. Savostianova, Phys. Rev. B **74**, 045325 (2006).